

Effect of Al₂O₃ Buffer Layers on the Properties of Sputtered VO₂ Thin Films

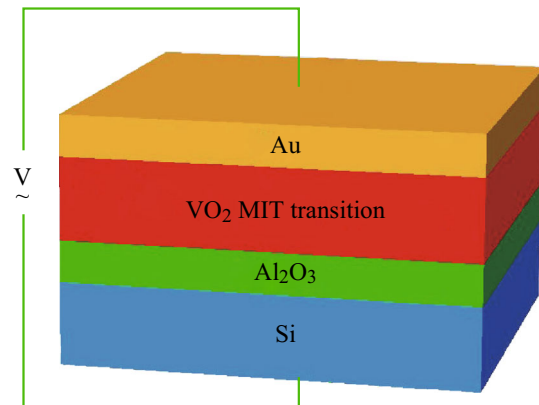
Dainan Zhang^{1,2} · Tianlong Wen¹ · Ying Xiong¹ · Donghong Qiu¹ · Qiye Wen¹

Received: 5 December 2016 / Accepted: 10 January 2017 / Published online: 14 February 2017
© The Author(s) 2017. This article is published with open access at Springerlink.com

Highlights

- High-quality VO₂ thin films were obtained on silicon substrates by introducing an Al₂O₃ buffer layer prepared by atomic layer deposition (ALD) under different growth conditions.
- The fast, electrically driven phase transition of VO₂ thin films was studied, and a possible mechanism was proposed according to the C–V measurement at a high frequency.

Abstract VO₂ thin films were grown on silicon substrates using Al₂O₃ thin films as the buffer layers. Compared with direct deposition on silicon, VO₂ thin films deposited on Al₂O₃ buffer layers experience a significant improvement in their microstructures and physical properties. By optimizing the growth conditions, the resistance of VO₂ thin films can change by four orders of magnitude with a reduced thermal hysteresis of 4 °C at the phase transition temperature. The electrically driven phase transformation was measured in Pt/Si/Al₂O₃/VO₂/Au heterostructures. The introduction of a buffer layer reduces the leakage current and Joule heating during electrically driven phase transitions. The C–V measurement result indicates that the phase transformation of VO₂ thin films can be induced by an electrical field.



Keywords Al₂O₃ · Buffer layers · Atomic layer deposition · VO₂ thin films · Heterostructure

Electronic supplementary material The online version of this article (doi:10.1007/s40820-017-0132-x) contains supplementary material, which is available to authorized users.

✉ Tianlong Wen
halong@uestc.edu.cn

¹ State Key Laboratory of Electronic Films and Integrated Devices, University of Electronic Science and Technology of China, Chengdu 610054, People's Republic of China

² Department of Electrical and Computer Engineering, University of Delaware, Newark, DE 19716, USA

1 Introduction

VO₂ thin films have generated a considerable interest among scientists over the past decades owing to their near-room-temperature phase transformation [1]. VO₂ thin films undergo transition from a reversible monoclinic (M phase) to a rutile (R phase) structural phase at approximately 65 °C, which is accompanied by a dramatic change in their electrical and optical properties [2–6]. The resistivity of

VO₂ thin films changes by three to five orders of magnitude during this phase transition. The metal-to-insulator (MIT) transition has been utilized in a variety of electronic devices such as electromagnetic wave modulators, switches [7–10], and holographic storage [11]. So far, the applications of VO₂ thin films have been mainly explored for infrared and millimeter waves [10, 12]. Recently, VO₂ thin films have been used for terahertz (THz)-wave devices [7]. In 2010, VO₂ nanowires were deposited on glass substrates using photolithography and magnetron sputtering and used for the thermal modulation of THz waves by Wen et al. [7]. The research results showed that the transmittance of THz waves reduced by 65% after traveling through VO₂ nanowire arrays during the MIT transition [7].

In 2013, VO₂ thin films with silver nanowire antenna arrays were deposited on a silicon substrate [13]. A reduction in the relative refractive index and a blue shift of the resonance frequency were observed, owing to changes in the dielectric constant of VO₂ thin films during heating [13]. Similarly, Seo et al. [8] created a rectangular hole array based THz wave antenna for controlling the transmittance of THz waves from 0.2 to 2 THz using the phase transition of VO₂ thin films.

VO₂ thin films have exhibited good potential for use in THz wave devices. However, compared to the electrical modulation in graphene [14–17] and the optical modulation in silicon [18–20], it is difficult to obtain a comparable response speed via the thermal modulation of THz waves using the phase transition of VO₂ thin films. Consequently, it is important to explore the fast phase transition of VO₂ thin films induced by an electrical field.

In many applications, the integration of VO₂ thin films with silicon technology and processing is desired, which requires the growth of VO₂ thin films on a silicon substrate [21]. However, there is a large lattice mismatch between the VO₂ thin films and silicon/silicon oxide substrates. The direct deposition of VO₂ thin films on silicon/silicon oxide often yields an inferior crystalline texture, resulting in a small change of resistivity and a large thermal hysteresis during MIT [21, 22]. Furthermore, the oxygen diffusion at the VO₂/Si interface adversely affects the quality of the deposited VO₂ thin films [22].

It has been proposed that using yttrium-stabilized zirconia (YSZ) as a buffer layer aids the growth of VO₂ thin films on a silicon substrate [21]. A YSZ buffer layer of 30–145 nm can reduce the thermal hysteresis temperature to 6 K and result in a resistance change of three orders of magnitude [21]. However, owing to the instability of the microstructure of YSZ, it is necessary to study a new buffer layer for VO₂ thin film deposition on a silicon substrate to achieve a better performance.

Previously, we used a dense Al₂O₃ thin film as the buffer layer to improve the quality of VO₂ thin films grown on a silicon substrate. This layer was grown via atomic layer deposition (ALD) [5]. The introduction of the Al₂O₃ buffer layer significantly improved the resistivity changes and the thermal hysteresis of VO₂ thin films during the MIT transition. An electrical-field-induced phase transformation was observed owing to the insulating Al₂O₃ layer.

However, it is challenging to obtain a pure phase of VO₂ in thin films, and much knowledge about the phase transformation of VO₂ is still unclear. Here, we have deposited VO₂ thin films under different conditions and investigated their optical and electrical properties. It was observed that the partial pressure of oxygen gas during sputtering has a significant impact on the phase of the deposited thin film. Pure VO₂ can be obtained on the Al₂O₃ buffer layer by optimizing the growth conditions. In contrast, it is difficult to obtain a pure VO₂ phase on a naked silicon substrate. In addition, the phase transformation induced by an electrical field was also studied. The capacitance–voltage curves indicate that the phase transformation occurs through the voltage-driven nucleation and the growth of metallic regions in VO₂ thin films. The high-quality VO₂ thin films grown on silicon substrates have great potential for applications in many functional devices.

2 Experimental Methods

In this study, p-type silicon (001) (with a resistivity ρ of approximately 1 Ω cm) was used as substrate, and cleaned by acetone, ethylene, and deionized water before deposition. The pretreated silicon substrate was loaded into a chamber for Al₂O₃ thin film deposition via plasma-enhanced atomic layer deposition (PEALD). Pure trimethylaluminum (TMA) was used as the precursor chemical. Al₂O₃ thin films with thicknesses ranging from 25 to 50 nm were deposited and used as the buffer layers for the growth of VO₂ thin films. Subsequently, the Al₂O₃-coated silicon substrate was transferred into a magnetron sputtering machine. In addition, naked silicon substrates were loaded into the same batch for comparison. Pure 4-inch vanadium (99.99%) was used as a target, and pure oxygen and argon gases were used as the reaction and sputtering gases. The base pressure was $<3 \times 10^{-4}$ Pa. During the deposition, the substrate temperature was maintained between 450 and 550 °C with a sputtering power of 200 W. VO₂ thin films with thicknesses ranging from 80 to 200 nm were obtained after a deposition time of 10–30 min. The chamber pressure was approximately 1 Pa. The partial pressure of oxygen varied from approximately 4–5%.

The deposited Al_2O_3 buffer layer and VO_2 thin films were evaluated using scanning electron microscopy (SEM, JSM-7600F), X-ray diffraction (XRD, DX-2700), and atomic force microscopy (AFM, SPA-300HV). Two gold electrodes of 1 mm separated by a distance of 6.5 μm were deposited to measure the in-plane resistivity. The silicon substrate was coated with platinum, and a gold pad with an area of $100 \times 100 \mu\text{m}^2$ was deposited on the VO_2 thin films for perpendicular measurement. The electrical resistivity was measured via a standard four-point measurement method using a Keithley 2400 Source Meter. The I - V curve and the capacitance as a function of voltage and frequency were measured using an Agilent 4156C system.

3 Results and Discussion

Al_2O_3 thin films deposited via PEALD were dense, smooth, with a clear interface, and high dielectric constant (i.e., k of approximately 8.8). They were thermally and chemically stable. Furthermore, the quality of the VO_2 thin film was significantly improved by depositing it on the Al_2O_3 buffer layer. A 3D AFM image of the Al_2O_3 thin film is shown in Fig. S1. The roughness of the deposited Al_2O_3 films was approximately 0.2 nm, which is comparable with that of the polished silicon substrates. In our study, Al_2O_3 thin films with a thickness of 25 nm were used as the buffer layers for VO_2 thin film deposition.

Figure 1 shows the SEM images of the sputtered VO_2 thin films on a silicon substrate and on the deposited Al_2O_3 buffer layers at different magnifications. It was observed that both the VO_2 thin films were polycrystalline but with different microstructures. The grains of the VO_2 thin films grown on the silicon substrate were small, irregular, and nonuniform in size. In contrast, the grains of the VO_2 thin films grown on the Al_2O_3 buffer were large, smooth, dense, and uniform in size. In the case of polycrystalline VO_2 thin films, the phase transformation can be affected by their crystallinity, grain size, density, and grain boundaries [23]. The discontinuous phase transformation is mainly caused by the energy barriers imposed by the grain boundaries [23]. Consequently, larger and denser grains benefit the phase transformation of the VO_2 thin films, and they were obtained in this work by introducing the Al_2O_3 buffer layer, as shown in Fig. 1.

Vanadium has multiple valence states (+2, +3, +4, and +5) in oxides, which is a challenge for obtaining a pure phase of VO_2 thin films. In our experiment, we observed that there was only a small window for the oxygen partial pressure to produce pure VO_2 thin films on the Al_2O_3 buffer layer. A slight difference in oxygen pressure during magnetron sputtering can significantly affect the phase of the deposited VO_x thin films. In this study, oxygen partial pressures of 4% and 5% were used to demonstrate their impact on the VO_2 thin films.

Figure 2a, b show the XRD patterns of two sets of samples prepared under oxygen pressures of 5% and 4%,

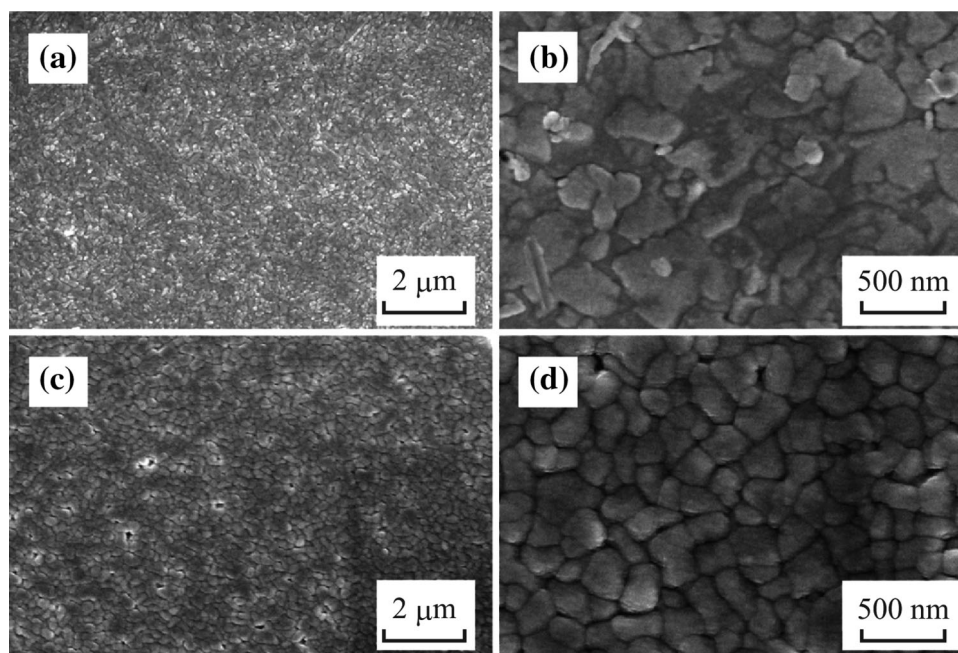


Fig. 1 SEM images of VO_2 thin films: **a, b** deposited on p-Si substrate, and **c, d** deposited on Al_2O_3 buffer layers. Here, **a, c** are shown in low magnification, and **b, d** are shown in high magnification

respectively. In the case of oxygen partial pressure of 5%, VO₂ thin films were obtained both on silicon and Al₂O₃ buffer layer. On a naked silicon substrate, V₆O₁₃ and V₂O₅ phases were also observed and the growth of the VO₂ phase was significantly suppressed. In contrast, the growth of VO₂ thin films was enhanced on the Al₂O₃ buffer layer, and the V₂O₅ phase was indiscernible by XRD for oxygen partial pressures of 5% and 4%. However, a small amount of V₆O₁₃ phase was still observed.

The undesired phases of V₆O₁₃ and V₂O₅ were oxygen rich as compared to the desired VO₂ phase. Consequently, the oxygen partial pressure was reduced to 4% during the magnetron sputtering. On the naked silicon substrate, the V₂O₅ phase was not discernible for the reduced oxygen partial pressure. Although a small amount of V₆O₁₃ phase was still present in the deposited thin films, the growth of the VO₂ phase was highly enhanced compared to the deposition at the oxygen partial pressure of 5%. Moreover, a pure VO₂ phase was obtained for the thin films deposited on the Al₂O₃ buffer layer at the oxygen partial pressure of 4%, and the growth of the VO₂ phase in the (011) direction was highly enhanced, which was evident from the high intensity of the (011) diffraction peak.

The enhanced VO₂ growth on the Al₂O₃ buffer layer could be the result of the reduced lattice mismatches and

the oxygen diffusion at the Al₂O₃/VO_x interface. The XRD patterns did not show signatures of the ALD-deposited Al₂O₃ thin films, indicating the amorphous nature of the buffer layers, which is consistent with previous research results [24, 25]. The amorphous Al₂O₃ buffer layer did not strain the lattice of the VO₂ thin films during growth, unlike naked silicon. Therefore, the VO₂ thin films grown on the Al₂O₃ buffer layers were much more homogenous than those grown on the silicon substrate, as shown in Fig. 1. Further, the Al₂O₃ buffer layers promoted texture growth along the (011) direction, which was also reported by other groups [26, 27].

Further, the Al₂O₃ buffer layer was chemically stable, preventing the interdiffusion of oxygen at the Al₂O₃/VO₂ interface. Oxygen atoms can easily diffuse at the Si/VO₂ interface at 450–550 °C, which renders the control of the stoichiometric composition of the VO₂ thin films difficult. Therefore, by introducing the Al₂O₃ buffer layer on a silicon substrate, the microstructure and stoichiometric composition were easier to control, resulting in higher quality VO₂ thin films. Notably, pure VO₂ thin films can also be deposited by magnetron sputtering from a vanadium target by carefully controlling the growth conditions [27]. However, the use of the Al₂O₃ buffer layer renders the deposition window wider and the electrical properties stronger, which will be discussed later.

The thermally induced phase transformations were investigated under different deposition conditions and microstructures. The sheet resistance of the thin films was measured as a function of temperature. The results are shown in Fig. S2 (oxygen partial pressures of 5%) and Fig. S3 (oxygen partial pressures of 4%). Table 1 lists the sheet resistances of the samples at 25 and 85 °C, and the transition temperatures during heating and cooling, which are calculated from Fig. S2 and Fig. S3. The resistivity ratio of the thin films before ($T = 25$ °C) and after ($T = 25$ °C) phase transition were significantly improved when deposited on the Al₂O₃ buffer layers over a naked silicon substrate, owing to the high resistivity of the thin films at room temperature (25 °C).

As shown in Table 1, the sheet resistance of the thin films deposited on the naked silicon was much smaller than that on the Al₂O₃ buffer layer, which could be the result of the presence of the V₆O₁₃ phase. The V₆O₁₃ phase undergoes an MIT transition at -123 °C, and it is in a metallic state at room temperature [28]. In Fig. 2, the thin films possessed a significant amount of V₆O₁₃ phase when deposited on the naked silicon, whereas the growth of V₆O₁₃ was suppressed when deposited on the Al₂O₃ buffer layer. The resistivity changes in the VO₂ thin films were further increased during the phase transition when deposited at the oxygen partial pressure of 4%. In addition, the temperature of thermal hysteresis was reduced from 9 °C

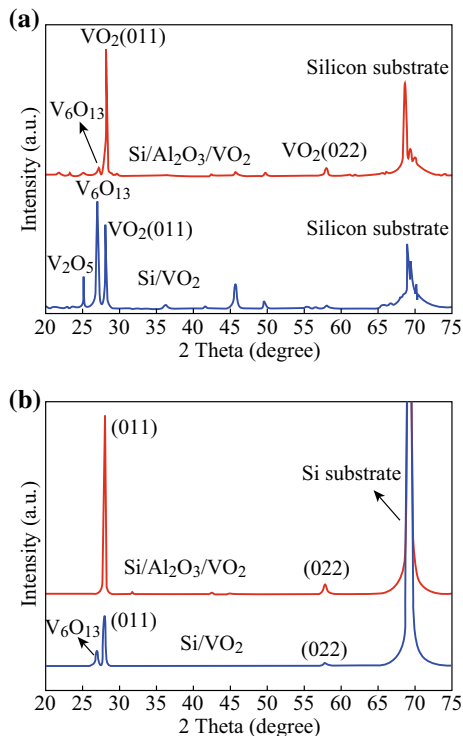


Fig. 2 X-ray θ - 2θ scan of VO₂ thin films grown on silicon and Al₂O₃ buffer layers under oxygen partial pressure of 5%, and 4% in **a** and **b**, respectively

Table 1 Sheet resistance and phase transformation temperature

Sample	PO ₂ (%)	$\rho_{25\text{ }^\circ\text{C}}$ (k Ω /sq)	$\rho_{85\text{ }^\circ\text{C}}$ (k Ω /sq)	$\rho_{25\text{ }^\circ\text{C}}/\rho_{85\text{ }^\circ\text{C}}$	T_{Cool} (°C)	T_{Heat} (°C)	ΔT (°C)
Si/VO ₂	5	4.5	0.025	180	56	65	9
	4	23	0.034	676	51.5	59.5	8
Si/Al ₂ O ₃ /VO ₂	5	169	0.07	2414	57	63	6
	4	106	0.013	8153	56	60	4

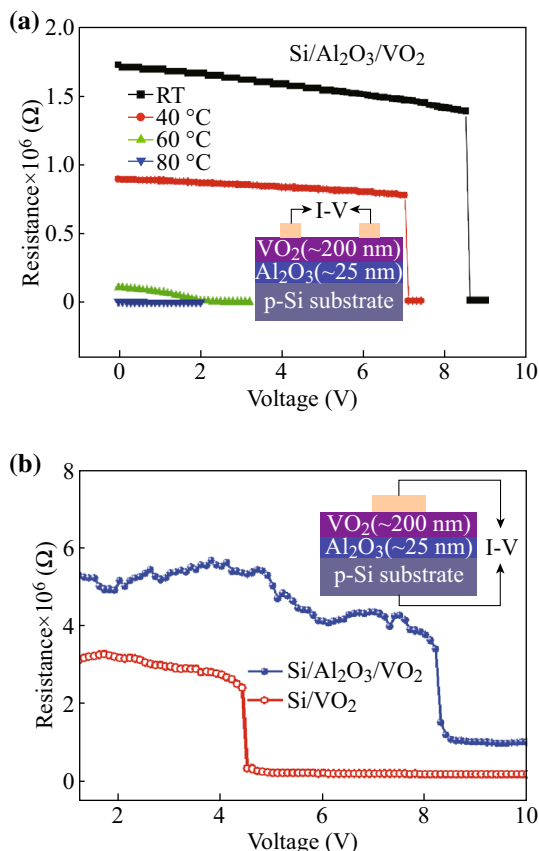


Fig. 3 **a** Resistance of VO₂ thin films on Al₂O₃ buffer layers measured along the in-plane direction, and **b** the resistance measured along the perpendicular direction for VO₂ thin films deposited on Al₂O₃ buffer layers and naked silicon substrate

on the naked silicon to 4 °C on the Al₂O₃ buffer layer at the oxygen partial pressure of 4%.

Electrodes were deposited on Si/Al₂O₃/VO₂ to investigate the electrically driven phase transformation. The resistance of the VO₂ thin films was measured along the in-plane and perpendicular directions, as shown in the insets of Fig. 3a, b, respectively. Two gold electrodes of 1 mm, separated by 6.5 μm, were deposited via thermal evaporation for the in-plane measurement. The Al₂O₃ buffer layers could prevent current leakage through the p-Si. At room temperature, the resistance had a magnitude of 10⁶ Ω when no bias was applied to the electrodes. As the voltage

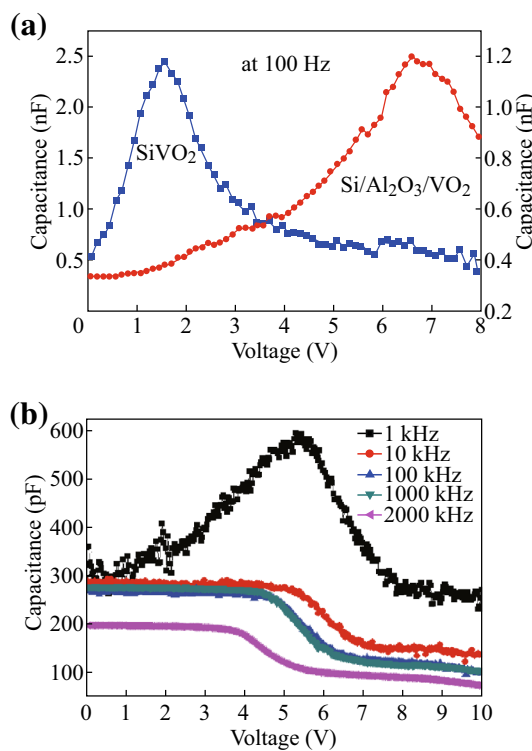


Fig. 4 **a** Capacitance of Pt/Si/Al₂O₃/VO₂/Au and Pt/Si/VO₂/Au stacks as a function of voltage at 100 Hz, and **b** capacitance of Pt/Si/Al₂O₃/VO₂/Au stacks as a function of voltage at different frequencies

bias was increased from 0 V, initially the resistance decreased gradually. However, when the voltage approached 8.5 V, an abrupt decrease of resistance was observed at room temperature, indicating a phase transformation.

Furthermore, an electrically driven phase transition was observed as the environmental temperature was increased to 40 °C, but the thermally induced phase transformation still did not occur. However, the resistivity was small at 40 °C than that at room temperature. Further, the switching voltage was reduced to approximately 7 V, which was lower than the value at room temperature. Therefore, thermal energy can assist the electrically driven phase transformation of VO₂ thin films. When the environmental temperature approached the value of the thermal phase transformation temperature at 60 °C, the resistance change during the electrically driven phase transition was very

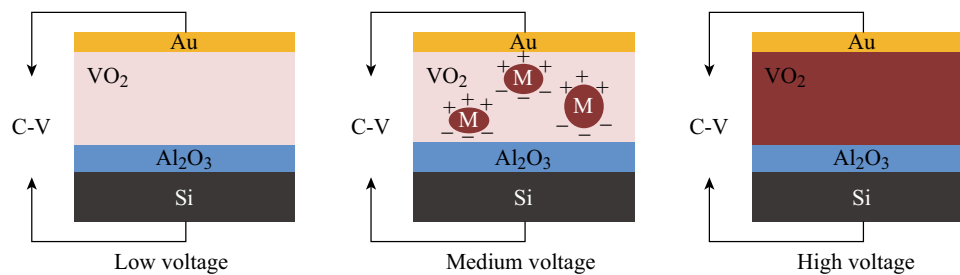


Fig. 5 Schematic mechanism of electrically driven phase transformation of VO₂ thin films

small, as shown by the green curves in Fig. 3a. At 80 °C, the VO₂ thin films were in metallic states, and no abrupt change in resistance was observed. Notably, the switching voltage monotonically decreased as the temperature increased.

The electrically driven phase transformation could be a result of the applied electrical field or Joule heating. In this regard, we are prone to believe that the phase transformation was induced by the applied electrical field. For verification, we measured the resistance of the VO₂ thin films along the perpendicular direction, as shown in the inset of Fig. 3b. The insulating Al₂O₃ buffer layer could effectively decrease the electrical current passing through the VO₂ thin films. The resistance was measured as a function of the applied voltage, as shown in Fig. 3b. The phase transformation occurred at 8.4 V for the Pt/Si/Al₂O₃/VO₂/Au stack, and at 4.4 V for the Pt/Si/VO₂/Au stack.

In Fig. 3a, the resistance of VO₂ is negligible after the phase transformation. Therefore, we estimated that the apparent resistances of the silicon substrate, Al₂O₃ buffer layer, and VO₂ thin films immediately before the phase transformation were 2×10^5 , 8×10^5 , and 3×10^6 Ω, respectively. A switching electrical field of 3×10^7 V m⁻¹ for the Pt/Si/Al₂O₃/VO₂ stack was estimated. When the VO₂ thin films were deposited on the silicon substrate, their resistance was estimated to be 2.45×10^6 Ω before the phase transformation, and the switching electrical field was 2×10^7 V m⁻¹. The decrease in the switching field of the Pt/Si/VO₂/Au stack could be a result of the microstructure of the deposited thin films.

In order to further investigate the electrically driven phase transformation of the VO₂ thin films, the capacitances of the Pt/Si/Al₂O₃/VO₂/Au and Pt/Si/VO₂/Au stacks were measured under an alternating field at 100 Hz. The result is shown in Fig. 4a. As the voltage increased, the capacitance of both the stacks increased and subsequently decreased, with a maximum value observed at 1.5 V for Pt/Si/VO₂/Au and at 6.8 V for Pt/Si/Al₂O₃/VO₂/Au. The capacitance–voltage curves were very different from those of typical MOS capacitors. We attribute this unusual behavior to the electrically driven phase transformation of the VO₂ thin films. As the voltage increased, some regions

of the VO₂ thin films were transformed from insulating to metallic.

Figure 5 shows the charge carriers were delocalized in the metallic region and oscillated with the AC field. It resulted in an increase in the dielectric constant of the VO₂ thin films. As the metallic region was percolated at high voltages, the capacitance decreased. The maximum capacitance during the phase transformation, which were triggered by temperature [29], was also observed in other MIT transitions. As shown in Fig. 4a, the nucleation and growth of the conducting regions can be induced gradually via a fast charge carrier injection during the AC oscillation [30]. These regions became conductive as percolation was achieved.

The capacitance of the Pt/Si/Al₂O₃/VO₂/Au stack was also measured as a function of voltage at different frequencies, as shown in Fig. 4b. At 1 kHz, the maximum capacitance was observed at a lower voltage of 5.2 V compared to the corresponding voltage value observed at 100 Hz. As the frequency of the AC field increased to 10 kHz, the maximum capacitance disappeared as the voltage increased, indicating that the oscillation of the charge carriers in the metallic regions could not match the AC field. The electrically driven phase transition of the VO₂ thin films can occur within 10 μs [31, 32]. The longer response time in our experiment could be a result of the large time constant RC owing to the presence of the Al₂O₃ layer. However, the phase transformation, indicated by the drop in capacitance, shifted to lower voltages as the frequency increased. This could be the result of easier nucleation of the new phase at high frequencies.

4 Conclusions

Al₂O₃ thin films were used as buffer layers to improve the growth of VO₂ thin films on silicon substrate. Pure VO₂ phases were obtained by depositing on the Al₂O₃ buffer layer at an oxygen partial pressure of 4%. Accordingly, a large resistance change and a small hysteresis were obtained for the thermally induced phase transformation. Furthermore, the electrical-field-induced phase transformation of

VO₂ thin films was also investigated. By measuring the capacitance at different voltages and frequencies, we propose that the phase transformation was initialized by the formation of metallic regions in the insulating VO₂ matrix. Our work provides a facile method to deposit VO₂ thin film on silicon substrate, which paves the way for fabricating VO₂-based devices such as fast electrical modulation of THz waves.

Acknowledgements This work was financially supported by the National Natural Science Foundation of China (Nos. 51401046, 51572042, 61131005, 61021061, and 61271037); International Cooperation Projects (Nos. 2013HH0003 and 2015DFR50870); the 111Project (No. B13042); the Sichuan Province S&T program (Nos. 2014GZ0003, 2015GZ0091, and 2015GZ0069); Fundamental Research Funds for the Central Universities; and the start-up fund from the University of Electronic Science and Technology of China.

Open Access This article is distributed under the terms of the Creative Commons Attribution 4.0 International License (<http://creativecommons.org/licenses/by/4.0/>), which permits unrestricted use, distribution, and reproduction in any medium, provided you give appropriate credit to the original author(s) and the source, provide a link to the Creative Commons license, and indicate if changes were made.

References

1. F.J. Morin, Oxides which show a metal-to-insulator transition at the Neel temperature. *Phys. Rev. Lett.* **3**(1), 34–36 (1959). doi:10.1103/PhysRevLett.3.34
2. Y. Muraoka, Z. Hiroi, Metal-insulator transition of VO₂ thin films grown on TiO₂ (001) and (110) substrates. *Appl. Phys. Lett.* **80**(4), 583–585 (2002). doi:10.1063/1.1446215
3. H.T. Zhang, L. Zhang, D. Mukherjee, Y.X. Zheng, R.C. Haislmaier, N. Alem, R. Engel-Herbert, Wafer-scale growth of VO₂ thin films using a combinatorial approach. *Nat. Commun.* **6**, 8475 (2015). doi:10.1038/ncomms9475
4. M. Eslamian, Inorganic and organic solution-processed thin film devices. *Nano-Micro Lett.* **9**, 3 (2017). doi:10.1007/s40820-016-0105-5
5. Y. Xiong, Q.Y. Wen, Z. Chen, W. Tian, T.L. Wen, Y.L. Jing, Q.H. Yang, H.W. Zhang, Tuning the phase transitions of VO₂ thin films on silicon substrates using ultrathin Al₂O₃ as buffer layers. *J. Phys. D-Appl. Phys.* **47**(45), 455304 (2014). doi:10.1088/0022-3727/47/45/455304
6. S. Saitzek, F. Guinneton, G. Guirleo, L. Sauques, K. Aguir, J.R. Gavarrí, VO₂ thin films deposited on silicon substrates from V₂O₅ target: limits in optical switching properties and modeling. *Thin Solid Films* **516**(6), 891–897 (2008). doi:10.1016/j.tsf.2007.04.129
7. Q.Y. Wen, H.W. Zhang, Q.H. Yang, Y.S. Xie, K. Chen, Y.L. Liu, Terahertz metamaterials with VO₂ cut-wires for thermal tunability. *Appl. Phys. Lett.* **97**(2), 021111 (2010). doi:10.1063/1.3463466
8. M. Seo, J. Kyoung, H. Park, S. Koo, H.S. Kim et al., Active terahertz nanoantennas based on VO₂ phase transition. *Nano Lett.* **10**(6), 2064–2068 (2010). doi:10.1021/nl1002153
9. R.M. Briggs, I.M. Pryce, H.A. Atwater, Compact silicon photonic waveguide modulator based on the vanadium dioxide metal-insulator phase transition. *Opt. Express* **18**(11), 11192–11201 (2010). doi:10.1364/oe.18.011192
10. M.R. Hashemi, S.H. Yang, M. Jarrahi, T.Y. Wang, N. Sepulveda, *IEEE, 2015 IEEE International Symposium on Antennas and Propagation & Usnc/Ursi National Radio Science Meeting* (IEEE, New York, 2015), pp. 77–78
11. W. Roach, Holographic storage in VO₂. *Appl. Phys. Lett.* **19**(11), 453 (1971). doi:10.1063/1.1653769
12. M.M. Qazilbash, M. Brehm, B.G. Chae, P.C. Ho, G.O. Andreev et al., Mott transition in VO₂ revealed by infrared spectroscopy and nano-imaging. *Science* **318**(5857), 1750–1753 (2007). doi:10.1126/science.1150124
13. S.K. Earl, T.D. James, T.J. Davis, J.C. McCallum, R.E. Marvel, R.F. Haglund, A. Roberts, Tunable optical antennas enabled by the phase transition in vanadium dioxide. *Opt. Express* **21**(22), 27503–27508 (2013). doi:10.1364/oe.21.027503
14. Q. Mao, Q.Y. Wen, W. Tian, T.L. Wen, Z. Chen, Q.H. Yang, H.W. Zhang, High-speed and broadband terahertz wave modulators based on large-area graphene field-effect transistors. *Opt. Lett.* **39**(19), 5649–5652 (2014). doi:10.1364/OL.39.005649
15. B. Sensale-Rodriguez, R.S. Yan, M.M. Kelly, T. Fang, K. Tahy et al., Broadband graphene terahertz modulators enabled by intraband transitions. *Nat. Commun.* **3**, 780 (2012). doi:10.1038/ncomms1787
16. D.N. Zhang, D.D. Sun, Q.Y. Wen, T.L. Wen, J. Kolodzey, H.W. Zhang, Tuning the optical modulation of wideband terahertz waves by the gate voltage of graphene field effect transistors. *Compos. B* **89**, 54–59 (2016). doi:10.1016/j.compositesb.2015.10.049
17. Q. Wen, Y. Liu, J. Liu, T. Wen, Q. Yang, Z. Chen, Y. Jing, H. Zhang, Large-area graphene FET based broadband terahertz modulator, in *2016 41st International Conference on Infrared, Millimeter, and Terahertz waves (IRMMW-THz)* (2016). doi:10.1109/IRMMW-THz.2016.7758633
18. T. Vogel, G. Dodel, E. Holzhauser, H. Salzmänn, A. Theurer, High-speed switching of far-infrared radiation by photoionization in a semiconductor. *Appl. Opt.* **31**(3), 329–337 (1992). doi:10.1364/AO.31.000329
19. T. Wen, D. Zhang, Q. Wen, Y. Liao, C. Zhang et al., Enhanced optical modulation depth of terahertz wave by self-assembled monolayer of plasmonic gold nanoparticles. *Adv. Opt. Mater.* **4**(12), 1974–1980 (2016). doi:10.1002/adom.201600248
20. T. Wen, C. Zhang, Q. Wen, Y. L. Jing, H. Zhang, J. Li, W. Tian, Y. Li, Improve optical modulation depth of terahertz wave by monolayers of plasmonic nanoparticles, in *2016 41st International Conference on Infrared, Millimeter, and Terahertz waves (IRMMW-THz)* (2016). doi:10.1109/IRMMW-THz.2016.7758773
21. A. Gupta, R. Aggarwal, P. Gupta, T. Dutta, R.J. Narayan, J. Narayan, Semiconductor to metal transition characteristics of VO₂ thin films grown epitaxially on Si (001). *Appl. Phys. Lett.* **95**, 111915 (2009). doi:10.1063/1.3232241
22. D.H. Qiu, Q.Y. Wen, Q.H. Yang, Z. Chen, Y.L. Jing, H.W. Zhang, Electrically-driven metal-insulator transition of vanadium dioxide thin films in a metal-oxide-insulator-metal device structure. *Mater. Sci. Semicond. Process.* **27**, 140–144 (2014). doi:10.1016/j.mssp.2014.06.030
23. F. Beteille, L. Mazerolles, J. Livage, Microstructure and metal-insulating transition of VO₂ thin films. *Mater. Res. Bull.* **34**(14–15), 2177–2184 (1999). doi:10.1016/s0025-5408(99)00232-9
24. K. Kimoto, Y. Matsui, T. Nabatame, T. Yasuda, T. Mizoguchi, I. Tanaka, A. Toriumi, Coordination and interface analysis of atomic-layer-deposition Al₂O₃ on Si(001) using energy-loss near-edge structures. *Appl. Phys. Lett.* **83**(21), 4306–4308 (2003). doi:10.1063/1.1629397
25. B. Hoex, S.B.S. Heil, E. Langereis, M.C.M. van de Sanden, W.M.M. Kessels, Ultralow surface recombination of c-Si

- substrates passivated by plasma-assisted atomic layer deposited Al_2O_3 . *Appl. Phys. Lett.* **89**(4), 042112 (2006). doi:[10.1063/1.2240736](https://doi.org/10.1063/1.2240736)
26. T.D. Manning, I.P. Parkin, Atmospheric pressure chemical vapour deposition of tungsten doped vanadium (IV) oxide from VOCl (3), water and WCl (6). *J. Mater. Chem.* **14**(16), 2554–2559 (2004). doi:[10.1039/b403576n](https://doi.org/10.1039/b403576n)
27. Z. Yang, C. Ko, S. Ramanathan, Metal-insulator transition characteristics of VO_2 thin films grown on Ge (100) single crystals. *J. Appl. Phys.* **108**(7), 073708 (2010). doi:[10.1063/1.3492716](https://doi.org/10.1063/1.3492716)
28. B. Fisher, A. Ron, The thermoelectric power in the conductive phase of V_6O_{13} . *Solid State Commun.* **40**, 737–739 (1981). doi:[10.1016/0038-1098\(81\)90818-8](https://doi.org/10.1016/0038-1098(81)90818-8)
29. H.F. Hess, K. Deconde, T.F. Rosenbaum, G.A. Thomas, Giant dielectric constants at the approach to the insulator-metal transition. *Phys. Rev. B* **25**(8), 5578–5580 (1982). doi:[10.1103/PhysRevB.25.5578](https://doi.org/10.1103/PhysRevB.25.5578)
30. K. Appavoo, B. Wang, N.F. Brady, M. Seo, J. Nag, R.P. Prasankumar, D.J. Hilton, S.T. Pantelides, R.F. Haglund, Ultrafast phase transition via catastrophic phonon collapse driven by plasmonic hot-electron injection. *Nano Lett.* **14**(3), 1127–1133 (2014). doi:[10.1021/nl4044828](https://doi.org/10.1021/nl4044828)
31. J. Sakai, High-efficiency voltage oscillation in $\text{VO}(2)$ planer-type junctions with infinite negative differential resistance. *J. Appl. Phys.* **103**(10), 103708 (2008). doi:[10.1063/1.2930959](https://doi.org/10.1063/1.2930959)
32. H.T. Kim, B.J. Kim, S. Choi, B.G. Chae, Y.W. Lee, T. Driscoll, M.M. Qazilbash, D.N. Basov, Electrical oscillations induced by the metal-insulator transition in VO_2 . *J. Appl. Phys.* **107**(2), 023702 (2010). doi:[10.1063/1.3275575](https://doi.org/10.1063/1.3275575)